

See discussions, stats, and author profiles for this publication at: <https://www.researchgate.net/publication/5283406>

Unusual Mechanisms Can Dominate Reactions at Hyperthermal Energies: An Example from $\text{O}(^3\text{P}) + \text{HCl} \rightarrow \text{ClO} + \text{H}$

ARTICLE in JOURNAL OF THE AMERICAN CHEMICAL SOCIETY · AUGUST 2008

Impact Factor: 12.11 · DOI: 10.1021/ja803080q · Source: PubMed

CITATIONS

10

READS

29

6 AUTHORS, INCLUDING:



Amy Brunsvold

SINTEF

51 PUBLICATIONS 549 CITATIONS

SEE PROFILE

Unusual Mechanisms Can Dominate Reactions at Hyperthermal Energies: An Example from $\text{O}(^3P) + \text{HCl} \rightarrow \text{ClO} + \text{H}$

Jianming Zhang,[†] Jon P. Camden,[‡] Amy L. Brunsvold,[†] Hari P. Upadhyaya,[†] Timothy K. Minton,^{*,†} and George C. Schatz^{*,‡}

Department of Chemistry and Biochemistry, Montana State University, Bozeman, Montana 59717, and
Department of Chemistry, Northwestern University, Evanston, Illinois 60208-3113

Received April 25, 2008; E-mail: tminton@montana.edu; schatz@chem.northwestern.edu

Neutral–neutral reactions at hyperthermal collision energies (~ 20 to ~ 300 kcal mol^{−1}) occur frequently in extreme environments,¹ for example, when space vehicles and their exhaust gases collide with O and N₂ in the outer atmosphere of the Earth.² Because the energies of these collisions exceed many reaction barriers, unknown reaction pathways are open, and unfamiliar reaction dynamics may be commonplace. Despite the importance of these high energy collisions, detailed studies of the dynamics of hyperthermal neutral–neutral reactions have been limited by the difficulty of producing an intense source of fast neutrals. In this work, we present the first experimental study of the highly endothermic reaction $\text{O}(^3P) + \text{HCl} \rightarrow \text{ClO} + \text{H}$ ($\Delta H_0^\circ = 38.9$ kcal mol^{−1}). The experiments in combination with theoretical calculations identify two distinct reaction pathways, whose dynamics are determined by whether the H atom of the HCl is oriented toward or away from the incoming reagent O atom. Surprisingly, the dominant mechanism at high energies does not correspond to motion near the reaction path. This finding is a general feature of light-atom eliminations in hyperthermal reactions and should be applicable to a range of similar systems.

Detailed studies of the dynamics of hyperthermal neutral reactions have generally been limited to reactions where one of the reagents is H or D.³ Earlier attempts were made to understand such reactions by using fast atoms obtained in nuclear recoil, but these “hot-atom” studies were difficult to interpret and highly averaged.⁴ Since these earlier studies, the detailed dynamics of only one hyperthermal reactive system with two heavy atoms have been studied both experimentally and theoretically.⁵

Crossed-molecular-beams experiments were performed with an apparatus equipped with a hyperthermal source containing $\sim 80\%$ $\text{O}(^3P)$ and $\sim 20\%$ $\text{O}_2(^3\Sigma_g^-)$.^{5,6} Pulsed beams of velocity-selected O atoms were crossed at right angles with a pulsed, supersonic beam of HCl gas. ClO products were detected at $m/z = 51$ (ClO^+) with a rotatable mass spectrometer detector that collected number density distributions as a function of arrival time, $N(t)$; see Supporting Information (SI). These time-of-flight (TOF) distributions were collected at different detector angles and were integrated to give laboratory angular distributions $N(\Theta)$. Θ is the angle at which the ClO scatters with respect to the direction of the O atom beam.⁷ A forward convolution method was used to derive center-of-mass (c.m.) translational energy $P(E_T)$ and angular $T(\theta_{\text{c.m.}})$ distributions from the laboratory $N(t)$ and $N(\Theta)$ distributions.⁸

Quasi-classical trajectories were integrated on the ground-state triplet surface, $^3A''$, using direct dynamics with forces and energies generated on the fly at the B3LYP/6-31G** level (see SI).⁹ The calculations were performed with the reagent HCl molecules in their

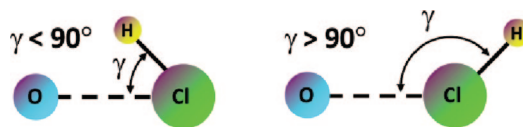


Figure 1. Gamma is defined as the angle between the O atom velocity vector and the H–Cl bond axis. The calculated reactive trajectories were sorted into two groups, one with $\gamma < 90^\circ$ and one with $\gamma > 90^\circ$.

lowest rotational state ($j = 0$), which approximates the experimental conditions where HCl is cooled to low rotational states in the supersonic expansion. The reactive trajectories were classified according to γ , which is the angle between the O atom velocity vector and the H–Cl bond axis when the reagents are well separated (Figure 1). We note that at the large relative velocities and low rotational states probed here γ remains constant during the interaction time of a collision.

Forward convolution fits to the laboratory TOF and angular distributions utilized two pairs of $P(E_T)$ and $T(\theta_{\text{c.m.}})$ distributions. ($\theta_{\text{c.m.}}$ is the angle between the velocity vectors of ClO and the reagent O in the c.m. frame; $\theta_{\text{c.m.}} = 0^\circ$ is defined as the forward direction.) To predict the laboratory data for each collision energy, one pair of $P(E_T)$ and $T(\theta_{\text{c.m.}})$ distributions was used for forward-scattered ClO, and a second pair of $P(E_T)$ and $T(\theta_{\text{c.m.}})$ distributions was used for backward-scattered ClO. It was impossible to fit the laboratory data with the use of a single pair of $P(E_T)$ and $T(\theta_{\text{c.m.}})$ distributions at a given collision energy. The experimentally derived distributions are shown in Figure 2a for a c.m. collision energy, E_{coll} , of 69.1 kcal mol^{−1}.

The experimental results thus lead to the conclusion that the forward-scattered ClO has a higher translational energy than the backward-scattered ClO. Laboratory data collected for higher collision energies exhibit analogous behavior and indicate that the fraction of ClO scattered in the forward direction increases with collision energy.

Theoretically derived $P(E)$ and $T(\theta_{\text{c.m.}})$ distributions show remarkable similarity to the experimentally derived distributions (Figure 2b). The calculations demonstrate that collisions with $\gamma < 90^\circ$ produce forward-scattered ClO with a relatively large release of translational energy, whereas collisions with $\gamma > 90^\circ$ produce backward-scattered ClO with less energy released in translation.

The experimental relative excitation function for ClO is shown normalized to the theoretical excitation function in Figure 3. Both theory and experiment agree that the cross section for the production of ClO rises from a threshold near 45 kcal mol^{−1} and reaches a maximum in the vicinity of 110 kcal mol^{−1}. Above this energy, theory shows that the cross section for ClO production decreases concomitantly with an increase in the cross section for producing $\text{H} + \text{Cl} + \text{O}$. Theory also reveals that collisions with $\gamma > 90^\circ$ lead

[†] Montana State University.

[‡] Northwestern University.

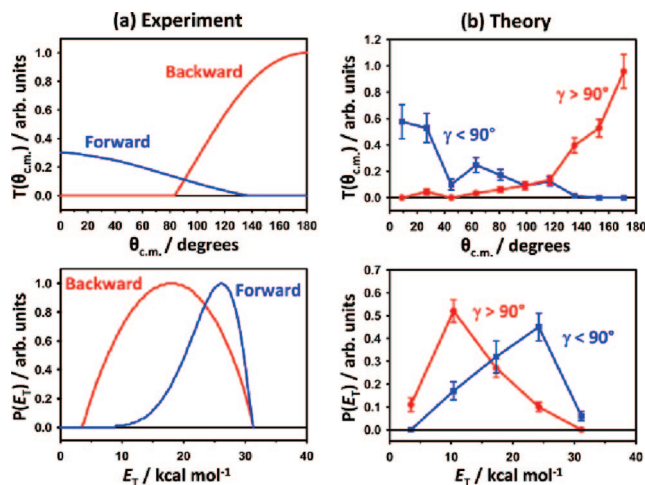


Figure 2. Center-of-mass translational energy and angular distributions derived from experiment (a) and theory (b). $\theta_{\text{c.m.}}$ is the scattering angle of the ClO product with respect to the O atom velocity vector, where $\theta_{\text{c.m.}} = 0^\circ$ is the forward direction. The experiment indicates that forward-scattered ClO is associated with large product relative translation, E_T , while backward-scattered ClO corresponds to smaller values of E_T . The theoretical calculations indicate that the forward-scattered ClO with large E_T corresponds to collisions with $\gamma < 90^\circ$, while backward-scattered ClO with small E_T corresponds to collisions with $\gamma > 90^\circ$.

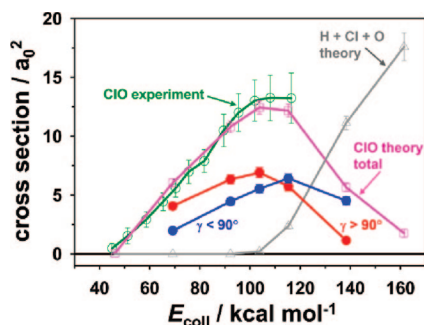


Figure 3. Experimental and theoretical excitation functions. The blue and red curves show components of the theoretical ClO excitation function, distinguished by trajectories with $\gamma < 90^\circ$ and $\gamma > 90^\circ$, respectively. While $\gamma > 90^\circ$ represents trajectories that follow closely the minimum energy path, a large fraction of the reactive trajectories is attributed to collisions with $\gamma < 90^\circ$, which are far from the minimum energy path.

to reaction with probabilities comparable to those for collisions with $\gamma < 90^\circ$, even at relatively low collision energies.

Our results suggest two distinctly different dynamical mechanisms for the $\text{O}(^3P) + \text{HCl} \rightarrow \text{ClO} + \text{H}$ reaction, animations of which may be seen in SI. The transition state at the threshold for producing ClO + H has a bent configuration, with an O–Cl–H angle of 158.0° , and is product-like.⁹ Collision geometries in which the H atom is oriented away from the incoming O atom ($\gamma > 90^\circ$) promote an $\text{S}_{\text{N}}2$ -like reaction, where the O atom collides with the Cl atom of the HCl molecule and the H atom is eliminated on the opposite side, traveling in roughly the same direction as the reagent O atom. The ClO product is therefore scattered in the backward direction with respect to the initial velocity of the reagent O atom. In this heavy + heavy-light (H + HL) mass combination, the H atom experiences a repulsive force that is relatively independent of the O–Cl bond length and is quickly ejected before the O–Cl bond length changes. Therefore, the H atom is eliminated with a translational energy that is determined by the repulsion from the OCl molecule regardless of the collision energy. Because the

maximum amount of translational energy of the H atom is limited,⁹ the energy partitioned into internal energy of ClO increases with collision energy, resulting in secondary dissociation of ClO at higher collision energies. Forward scattering of ClO results from trajectories that have collision geometries with small O–Cl–H angles, $\gamma < 90^\circ$. In these collision geometries, the H atom in the HCl molecule is oriented toward the reagent O atom, and the O atom interacts with both the Cl and H atoms. Therefore, as the Cl–O bond forms, the H atom experiences a strong repulsive force from both the O and Cl atoms, and it can carry away large translational energies as it is eliminated. The excitation function for production of ClO is the net result of both collision geometries and their relative cross sections. As the collision energy increases, the cross section for production of ClO increases until secondary dissociation of ClO starts to occur, and then this cross section decreases as the fraction of secondary dissociation trajectories increases. At higher collision energies ($> 110 \text{ kcal mol}^{-1}$), stable ClO is favored by trajectories with $\gamma < 90^\circ$, which scatter ClO into the forward direction, and the angular distribution of ClO shifts from mainly backward to mainly forward as the collision energy increases. The velocity distribution of ClO reflects the different scattering dynamics which lead to higher velocity ClO in the forward direction than in the backward direction. These dynamics are analogous to those inferred for the H atom elimination channel in the reaction of $\text{O}(^3P) + \text{H}_2\text{O}$,¹⁰ and they should be general for hyperthermal reactions in which a light product, such as an H atom, may be eliminated.

This study illustrates the important contribution of a reaction mechanism which does not involve motion near the minimum energy path. Motion along the minimum energy path can still occur, but at sufficiently high collision energies, such trajectories lead to dissociation and thus do not yield the primary reaction products, ClO + H. This unusual situation requires energies above the secondary dissociation threshold, but it should be common for hydrogen elimination reactions at hyperthermal collision energies.

Acknowledgment. This work was supported by the Air Force Office of Scientific Research (FA9550-04-1-0428 and FA9550-07-1-0095) and the Missile Defense Agency under Cooperative Agreement HQ0006-05-2-0001. A.L.B. is grateful for fellowships from the Zonta Foundation and the Montana Space Grant Consortium.

Supporting Information Available: TOF distributions of ClO collected at a variety of collision energies. Animated trajectories of the title reaction. This material is available free of charge via the Internet at <http://pubs.acs.org>.

References

- (1) *Chemical Dynamics in Extreme Environments*; Dressler, R., Ed.; Advanced Series in Physical Chemistry11; World Scientific: Singapore, 2001.
- (2) Murad, E. J. *Spacecr. Rockets* **1996**, *33*, 131.
- (3) Pomerantz, A. E.; Camden, J. P.; Chiou, A. S.; Ausfelder, F.; Chawla, N.; Hase, W. L.; Zare, R. N. *J. Am. Chem. Soc.* **2005**, *127*, 16368.
- (4) Tominaga, T.; Tachikawa, E. *Modern Hot Atom Chemistry*; Springer-Verlag: Heidelberg, 1981.
- (5) Brunsvold, A. L.; Upadhyaya, H. P.; Zhang, J.; Cooper, R.; Minton, T. K.; Braunstein, M.; Duff, J. W. *J. Phys. Chem. A* **2008**, *112*, 2192.
- (6) Garton, D. J.; Brunsvold, A. L.; Minton, T. K.; Troya, D.; Maiti, B.; Schatz, G. C. *J. Phys. Chem. A* **2006**, *110*, 1327.
- (7) A rotation of the detector toward the HCl beam corresponds to a positive increase in Θ .
- (8) (a) Lee, Y. T. *Reactive Scattering I: Nonoptical Methods*. In *Atomic and Molecular Beam Methods*; Scoles, G., Ed.; Oxford University Press: New York, 1988; Vol. 1; p 553. (b) Buss, R. J., Ph.D. Thesis, University of California, 1979.
- (9) Camden, J. P.; Schatz, G. C. *J. Phys. Chem. A* **2006**, *110*, 13681.
- (10) Brunsvold, A. L.; Zhang, J.; Upadhyaya, H. P.; Minton, T. K.; Camden, J. P.; Paci, J. T.; Schatz, G. C. *J. Phys. Chem. A* **2007**, *111*, 10907.

JA803080Q